Magnetic field effects in carbon nanotubes

2007 J. Phys.: Condens. Matter 19 395017

(http://iopscience.iop.org/0953-8984/19/39/395017)

IOP PUBLISHING JOURNAL OF PHYSICS: CONDENSED MATTER

J. Phys.: Condens. Matter **19** (2007) 395017 (10pp) doi:10.1088/0953-8984/19/39/395017

Magnetic field effects in carbon nanotubes

S Bellucci[1], J González[2], F Guinea[3], P Onorato[1,4] and E Perfetto[1,5]

[1] INFN, Laboratori Nazionali di Frascati, PO Box 13, 00044 Frascati, Italy
[2] Instituto de Estructura de la Materia, Consejo Superior de Investigaciones Científicas, Serrano 123, 28006 Madrid, Spain
[3] Instituto de Ciencia de Materiales, Consejo Superior de Investigaciones Científicas, Cantoblanco, 28049 Madrid, Spain
[4] Department of Physics 'A Volta', University of Pavia, Via Bassi 6, I-27100 Pavia, Italy
[5] Consorzio Nazionale Interuniversitario per le Scienze Fisiche della Materia, Universita' di Roma Tor Vergata, Via della Ricerca Scientifica 1, 00133 Roma, Italy

Received 28 February 2007, in final form 15 March 2007
Published 30 August 2007
Online at stacks.iop.org/JPhysCM/19/395017

Abstract

We study the effects of a perpendicular magnetic field on the transport properties of carbon nanotubes. For values of the magnetic length smaller than the curvature radius, the system displays well-defined Landau levels and an integer quantum Hall effect. The localized Gaussian Landau states develop in the central region of the nanotube surface, where the component of the magnetic field is maximum. Conversely, chiral currents flow at the flanks of the nanotube, producing a quantization of the Hall conductivity by even multiples of $2e^2/h$. Remarkably, it differs from the quantization rule by odd multiples of $2e^2/h$ recently found in planar graphene. Finally, the effects of the electron–electron interaction in the quantum Hall regime are considered. It is shown that the localization of chiral currents on opposite sides of the system reflects a strong suppression of back-scattering, enhancing the tunnelling density of states.

1. Introduction

The recent observation of the integer quantum Hall effect in planar graphene [1, 2] has attracted much attention on the effects of a perpendicular magnetic field in two-dimensional (2D) carbon compounds. In these systems the sp^2 bonding produces the arrangement of the carbon atoms in a honeycomb lattice, giving rise to electron quasiparticles with conical dispersion around discrete Fermi points. This seems to be at the origin of remarkable features of the resistivity as well as of the Hall conductivity, which in planar graphene is quantized according to [3, 4]

$$\sigma_{xy} = 2\frac{e^2}{h}(2n+1). \tag{1}$$

Carbon nanotubes can also be considered as the result of wrapping up a graphene sheet, leading to quasi-one-dimensional systems where the transport seems to be ballistic under certain conditions [5], as a consequence of the suppression of the scattering between different

low-energy subbands [6, 7]. The low-energy electronic states of both metallic carbon nanotubes and graphene sheets are characterized by linear dispersion around the Fermi points, with the result that they are governed by a two-component massless Dirac equation [8–10].

In this paper we investigate the effects of a transverse magnetic field on the transport properties of carbon nanotubes by looking at the possibility of forming Landau levels and *edge* states in such closed geometry. While the effect of a magnetic field parallel to the tube axis is well known, the transport properties of carbon nanotubes under a transverse magnetic field are less well understood [11]. We will see that carbon nanotubes of sufficiently large radius may also have a quantum Hall regime, with a quantized Hall conductivity σ_{xy}. We will find that the different topology of the carbon nanotubes with respect to planar graphene leads to a quantization in even steps of the quantity $2e^2/h$.

For the Hall regime to arise, the radius R of the nanotubes has to be larger than the magnetic length $\ell = \sqrt{\hbar c/eB}$, since this is the typical size of the localized states in Landau levels. Suitable conditions can be already found in thick multi-walled nanotubes for magnetic fields $B \gtrsim 1$ T, which correspond to magnetic lengths $\ell \lesssim 30$ nm. We will see that, for $\ell < R$, the eigenstates of the carbon nanotube organize into incipient Landau subbands, with a highly degenerated level at zero energy. The branches with linear dispersion correspond to states localized at the flanks of the nanotube, carrying quantized currents which are responsible for the conductivity along the longitudinal dimension of the nanotube.

The plan of the paper is the following. In section 2 we introduce a tight-binding model suitable for zig-zag carbon nanotubes in the presence of a transverse magnetic field B. On this basis we derive a simple field theory of Dirac spinors coupled to a gauge field. In section 3 we present numerical results for the band structure by varying the strength of the magnetic field B. We show that Landau levels develop when the magnetic length is comparable to the radius and study the spatial distribution of the corresponding eigenfunctions. The quantization rule for the Hall conductivity is derived in section 4, where a comparison to the case of planar graphene is also carried out. In the section 5 we introduce the effects of the Coulomb interaction between electrons, showing that the spatial localization of the electron modes induces a strong enhancement of the tunnelling density of states. Finally, the main conclusions are drawn in section 6.

2. Tight-binding model in the presence of a perpendicular magnetic field

In order to establish a relation with the quantum Hall effect in graphene, it is convenient to set up an approach focusing on the features of the states over distances much larger than the C–C distance a. The low-energy band structure can be obtained in graphene by taking a continuum limit in which the momenta are much smaller than the inverse lattice spacing $1/a$ [8–10]. In the case of carbon nanotubes under a magnetic field, a sensible continuum limit requires also that $\ell \gg a$, so that lattice effects can be disregarded.

We illustrate the long-wavelength limit in the case of zig-zag nanotubes, having in mind that different chiralities can be studied in a quite similar way. The tight-binding model for zig-zag nanotubes can be set up by considering a unit cell with length $3a$, that contains four transverse arrays of carbon atoms at different longitudinal positions x_j, $j = 1, \ldots 4$. We introduce the Fourier transform of the electron operator $\Psi(x_j, n)$ with respect to the position of the carbon atoms $n = 1, 2, \ldots N$ in each transverse section (see figure 1)

$$\Psi(x_j, n) \sim \sum_p \mathrm{e}^{\mathrm{i}2\pi np/N} \Psi_p(l; j) \tag{2}$$

where $l \in Z$ runs over the different cells. The index p labels the different 1D subbands, $p = 0, \pm 1, \ldots \pm (N-1)/2$ (or $N/2$) for the case of odd (even) N.

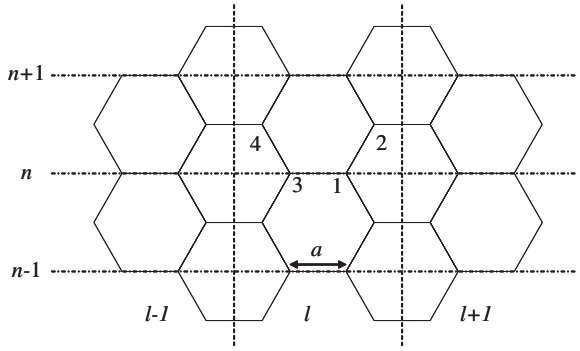

Figure 1. Illustration of the honeycomb lattice for zig-zag nanotubes.

The magnetic field is introduced with the usual prescription of correcting the transfer integral by appropriate phase factors

$$\exp\left(\mathrm{i}\frac{e}{\hbar c}\int_{\mathbf{r}}^{\mathbf{r}'}\mathbf{A}\cdot\mathbf{dl}\right) \tag{3}$$

depending on the vector potential $\mathbf{A}$ between nearest-neighbour sites $\mathbf{r}$ and $\mathbf{r}'$. In our case the vector potential has been chosen with the appropriate functional dependence at the nanotube surface, so that the phase factor becomes $a(e/\hbar c)BR\sin(2\pi n/N)$ [11]. In the continuum limit characterized by $(e/\hbar c)BRa \ll 1$, we may deal with the linear approximation in magnetic field strength, obtaining a tight-binding Hamiltonian

$$\begin{aligned}H_{\mathrm{tb}} = -t\Bigg(&\sum_{p,l} z_p d_p^+(l;1)d_p(l;2) + \sum_{p,l} d_p^+(l;3)d_p(l;1)\\ &+ \sum_{p,l} z_p^* d_p^+(l;4)d_p(l;3) + \sum_{p,l} d_p^+(l;2)d_p(l+1;4)\\ &\mp \frac{1}{4}\frac{eBRa}{\hbar c}\sum_{p,l} z_p d_p^+(l;1)d_{p\pm1}(l;2) \mp \frac{1}{2}\frac{eBRa}{\hbar c}\sum_{p,l} d_p^+(l;3)d_{p\pm1}(l;1)\\ &\mp \frac{1}{4}\frac{eBRa}{\hbar c}\sum_{p,l} z_p^* d_p^+(l;4)d_{p\pm1}(l;3)\\ &\mp \frac{1}{2}\frac{eBRa}{\hbar c}\sum_{p,l} d_p^+(l;2)d_{p\pm1}(l+1;4)\Bigg) + \mathrm{h.c.}\end{aligned} \tag{4}$$

where $d_p^{(+)}(l;j)$ is the annihilation (creation) of an electron in subband p on cell l and site j, t is the hopping integral and $z_p = 1 + \exp(\mathrm{i}2\pi p/N)$.

In the absence of magnetic field, each subband is obtained from the diagonalization of a 4×4 matrix describing the unit cell and reflecting the translational invariance in the longitudinal direction:

$$\mathcal{H}_{p,p'}\big|_{B=0} = \delta_{p,p'}\, t \begin{pmatrix} 0 & z_p^* & 1 & 0\\ z_p & 0 & 0 & \mathrm{e}^{\mathrm{i}3ka}\\ 1 & 0 & 0 & z_p^*\\ 0 & \mathrm{e}^{-\mathrm{i}3ka} & z_p & 0 \end{pmatrix} \tag{5}$$

where k denotes the longitudinal momentum. This leads in general to massive subbands with parabolic dispersion, with a gap $2\Delta_p = 2t|1 - 2\cos(\pi p/N)|$. We note that for $p = \pm N/3$

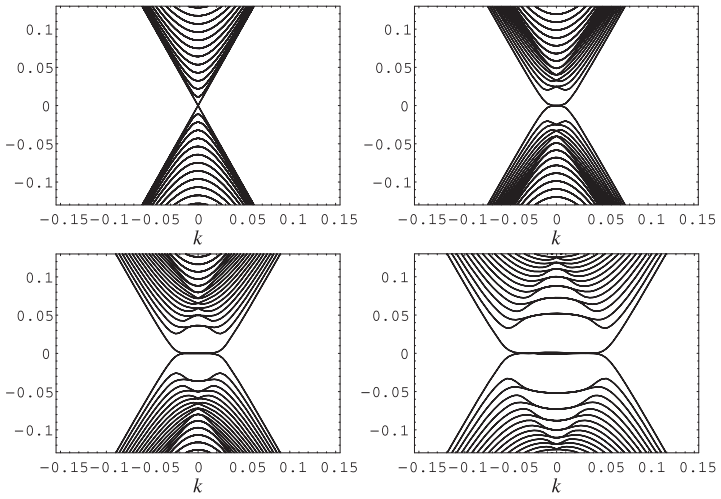

Figure 2. Band structure of a zig-zag nanotube in a transverse magnetic field, for a radius $R \approx 20$ nm and field strength $B = 0$ T (first panel); $B = 5$ T (second panel); $B = 10$ T (third panel); $B = 20$ T (fourth panel). $B = 20$ T corresponds to $aR/\ell^2 \approx 0.1$ and $R/\ell \approx 3.5$. Energy is in units of t and momentum is in units of Å^{-1}.

the gap vanishes and we get massless subbands crossing each other at zero energy (see figure 2 first panel, for an illustration). The dispersive branches can be decoupled from the high-energy branches that appear near the top of the spectrum. It turns out that the low-energy dispersion corresponds to a reduced two-component spinor described by the 2×2 Hamiltonian

$$\mathcal{H}_{p,p'}\big|_{B=0} = \delta_{p,p'} \begin{pmatrix} v_F \hbar k & \Delta_p \\ \Delta_p & -v_F \hbar k \end{pmatrix} \tag{6}$$

where the Fermi velocity is $v_F = 3ta/2\hbar$. The 2×2 structure of the Schrödinger equation gives rise to a two-component spinor $(\Psi_{p,R}, \Psi_{p,L})$. It appears that the two components of the spinor $\Psi_{p,R}$, $\Psi_{p,L}$ correspond respectively to right and left modes (note the corresponding opposite Fermi velocities in equation (6)), which are mixed by the massive (off-diagonal) term of the Hamiltonian.

The magnetic field introduces an interaction which is nondiagonal in the space of the different subbands, and that can be represented by the operator

$$\begin{aligned} \Delta\mathcal{H}_{p,p'} = {} & \delta_{p',p+1} t \frac{eBRa}{2\hbar c} \begin{pmatrix} 0 & -z_p/2 & 1 & 0 \\ z^*_{p+1}/2 & 0 & 0 & -e^{i3ka} \\ -1 & 0 & 0 & z_{p+1}/2 \\ 0 & e^{-i3ka} & -z^*_p/2 & 0 \end{pmatrix} \\ & + \delta_{p',p-1} t \frac{eBRa}{2\hbar c} \begin{pmatrix} 0 & z_p/2 & 1 & 0 \\ -z^*_{p-1}/2 & 0 & 0 & e^{i3ka} \\ -1 & 0 & 0 & -z_{p-1}/2 \\ 0 & -e^{-i3ka} & z^*_p/2 & 0 \end{pmatrix}. \end{aligned} \tag{7}$$

By projecting again onto the 2D low-energy space, $\Delta\mathcal{H}_{p,p'}$ becomes

$$\Delta\mathcal{H}_{p,p'} = \delta_{p',p\pm1} \begin{pmatrix} \pm i v_F (e/c) BR/2 & 0 \\ 0 & \mp i v_F (e/c) BR/2 \end{pmatrix}. \tag{8}$$

The Hamiltonian can be more easily expressed when acting on the two-component Dirac spinor

$$\Psi(k,\theta) \sim \sum_p \mathrm{e}^{\mathrm{i}\theta p}\Psi_p(k) \tag{9}$$

depending on the angular variable θ around the tubule. In this basis there are in fact two different sectors describing states with opposite angular momentum around the nanotube. The Hamiltonian is in either case

$$\mathcal{H} = \begin{pmatrix} v_{\mathrm{F}}\hbar k + v_{\mathrm{F}}\frac{eBR}{c}\sin(\theta) & \mathrm{i}(\hbar v_{\mathrm{F}}/a)\partial_\theta \\ \mathrm{i}(\hbar v_{\mathrm{F}}/a)\partial_\theta & -v_{\mathrm{F}}\hbar k - v_{\mathrm{F}}\frac{eBR}{c}\sin(\theta) \end{pmatrix} \tag{10}$$

where the periodic modulation matches with the orientation of a magnetic field normal to the nanotube surface at $\theta = 0$. Expression (10) actually corresponds to the Dirac Hamiltonian with the usual prescription for the coupling to the vector potential.

We have checked numerically that, as expected, the eigenstates of (10) provide a good approximation to the low-energy band structure of the carbon nanotubes for $aR/\ell^2 \ll 1$.

In the next section we will see that, for intermediate values of the magnetic length $\ell \sim R$, the spectrum starts to develop a flat Landau level at zero energy, in similar fashion as in the case of graphene.

3. Landau and current-carrying states

We have diagonalized the Hamiltonian (10) numerically for a nanotube with radius $R \approx 20$ nm and magnetic field B varying between 0 and 20 T. The corresponding band structure is shown in figure 2 (see also [12]). The plot corresponds to a zig-zag nanotube, but it can be shown that the shape of the band structure remains the same for other geometries, with the two valleys at zero energy (that appear superposed in figure 2) expanding in general around the two Fermi points of the system at $B = 0$. We see that flat Landau levels start developing already at $B = 10$ T (figure 2, third panel). For each momentum around $k = 0$ there is a four-fold degeneracy in the flat level. This extends into dispersive branches with particle- and hole-like character, at each side in momentum space. We have checked that for large B ($B = 20$ T, fourth panel) the energy levels at $k = 0$ follow the quantization rule $\varepsilon_n \propto \sqrt{n}$, which is peculiar to graphene [13]. The existence of a zero-energy level at $k = 0$ has been also shown to be a robust property of carbon nanotubes in a transverse magnetic field [14]. The point that we want to stress here is our observation that the levels at $k = 0$ are four-fold degenerate, including the zero-energy level, for any kind of nanotube geometry. As we will see, this bears a direct relation to the quantization of the Hall conductivity in even multiples of $2e^2/h$.

A remarkable physical insight is obtained by looking at the eigenfunctions of the Hamiltonian (10) when the Landau levels have already developed. In figure 3 we show the spatial distribution of the lowest Landau level (with finite although very small positive energy) for $B = 20$ T. We see that each eigenfunction of (10) is in general localized around a certain value of the angular variable θ. The zero-energy states at $k = 0$, for instance, have Gaussian wavefunctions localized at $\theta = 0$ or π, where the normal component of the magnetic field is maximum. Moreover (see figure 3 central panels), the left-component Ψ_{L} of the wavefunction exactly compensates the right-component Ψ_{R}. As a consequence we expect that such states around $k = 0$ do not carry any net current. This issue will be studied in more detail in the next section.

For positive [negative] longitudinal momentum, the zero-energy states have two Gaussian structures peaked in the intervals $(\pi, 3\pi/2)$ and $(3\pi/2, 2\pi)$ [$(0, \pi/2)$ and $(\pi/2, 3\pi/2)$]. Quite interestingly (see figure 3 top and bottom panels), the states in the dispersive branches have

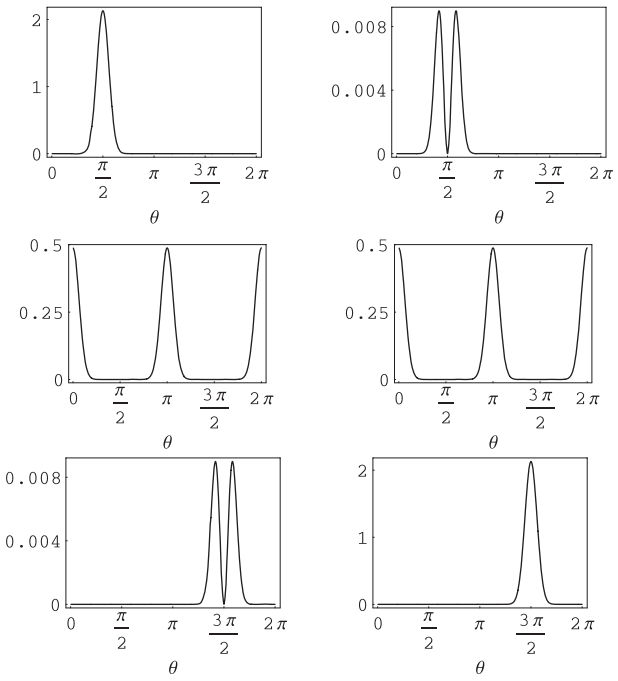

Figure 3. Angular distribution of the eigenfunctions in the lowest Landau level of a zig-zag nanotube in a transverse magnetic field, for a radius $R \approx 20$ nm and field strength $B = 20$ T. In the left (right) panels we plot $|\Psi_L|^2$ ($|\Psi_R|^2$) as a function of the angular variable θ, for different values of the longitudinal momentum k. From top to bottom we have $k = -0.15, 0, 0.15$ (in units of Å^{-1}). We note that $k \pm 0.15$ has been chosen in such a way that the corresponding eigenmodes are in the full linear regime of figure 2, fourth panel. The interpolation between the figures in three panels is smooth for intermediate values of k.

Gaussian wavefunctions (with a width that is proportional to $\sqrt{\ell}$) centred about $\pi/2$ (for a left branch) or $3\pi/2$ (for a right branch). In these regions the normal component of the magnetic field is vanishing, and therefore we expect the electrons to behave as if they were free. Here the role of the magnetic field is to separate left-moving and right-moving states at opposite sides of the tube. Indeed for these states there is a large mismatch between Ψ_L and Ψ_R, and they are expected to carry nonvanishing chiral currents flowing at the flanks of the nanotube.

The localization of the states in the dispersive branches at the flanks of the tubule suggests that, despite having no boundary, the carbon nanotube may support edge excitations in a similar fashion as in systems with planar geometry. To check this fact, one may compute the current flowing in the longitudinal direction for the different states.

4. Quantization rule for the Hall conductivity

In this section we show that the current carried in the longitudinal direction by the states in the outer dispersive branches is quantized. For Dirac spinors, the definition of the current follows from the continuity equation

$$\partial_t(\Psi_R^+\Psi_R + \Psi_L^+\Psi_L) = v_F\partial_x(\Psi_R^+\Psi_R - \Psi_L^+\Psi_L) \tag{11}$$

where Ψ_L and Ψ_R correspond to the same basis used to write the Dirac Hamiltonian (10).

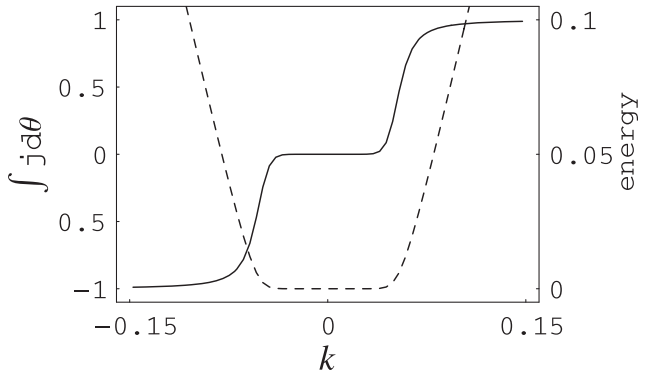

Figure 4. Plot of the integral of the current j over the angular variable θ as a function of the longitudinal momentum k (solid line), for states in the lowest Landau subband shown in figure 2. The energy dispersion of the subband is also shown (dashed line). Energy is in units of t and momentum is in units of Å^{-1}.

The result of computing the integral over θ of the current $j = \Psi_R^+ \Psi_R - \Psi_L^+ \Psi_L$ for the lowest energy subband is represented in figure 4. It turns out that, in general, the states corresponding to the flat part of the Landau level (displayed in figure 4 by the dashed line) do not carry any current in the longitudinal direction, while the states in the dispersive branches saturate quickly the unit of current as the dispersion approaches a constant slope.

The quantization of the current for the states in the dispersive branches opens the possibility to observe the quantization of the Hall conductivity in thick carbon nanotubes. In general, the quantization of the current is more accurate for smaller curvature of the dispersive branches. It happens moreover that, when the Fermi level crosses one of the bumps with parabolic dispersion shown in figure 2, the two contributions to the current from the respective Fermi points go in the opposite direction and tend to cancel each other. Envisaging an experiment where a potential difference is applied between the two flanks of a thick nanotube, we obtain that the current in the longitudinal direction is given approximately by the excess (or deficiency) of filled states in the right dispersive branches, with respect to those in the left dispersive branches. Making the equivalent of the arguments applied for planar geometries [15], we conclude that the Hall conductivity σ_{xy} must follow an approximate quantization rule, with a prefactor given by the spin degeneracy and the doubling of the subbands shown in figure 2:

$$\sigma_{xy} \approx 4\frac{e^2}{h}n. \tag{12}$$

In contrast to what happens in the case of graphene, we observe that the Hall conductivity is quantized in even steps of $2e^2/h$. It can be shown that this feature is a consequence of the vanishing net flux traversing the nanotube surface [16].

5. Effects of Coulomb interaction

The existence of extended states along the flanks of the nanotube also gives the insight to understand the effects of the electron–electron interaction in the presence of a magnetic field. At $B = 0$, the transport properties are dictated by the so-called Luttinger liquid behaviour, which is a reflection of the repulsive interaction in the nanotubes [6, 7]. When the magnetic field is switched on, however, the Coulomb interaction renormalizes, in a different manner, the Fermi velocity as well as the compressibility for the extended states near the Fermi level.

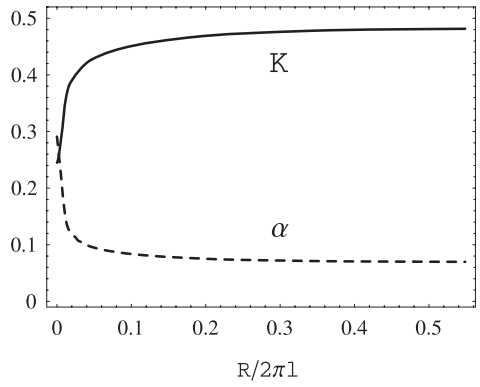

Figure 5. Plot of the Luttinger liquid parameter K (solid line) and of the critical exponent α (dashed line) as a function of $R/2\pi\ell$. Here the radius is fixed at $R \approx 20$ nm and B is ranging between 0 T ($\ell = \infty$) and 20 T ($\ell \approx 6$ nm).

Let us focus on the case where the Fermi level is right above (or below) the plateau at zero energy. The Fermi velocity is renormalized by the so-called g_4 coupling, given by the matrix element of the Coulomb interaction for electrons scattering near the same Fermi point (i.e. having the same chirality) [17]. This quantity can be computed using the eigenfunctions of the Dirac Hamiltonian (10). At the flanks of the nanotube, their wavefunctions have Gaussian shape, with a width that is proportional to $\sqrt{\ell}$. Thus, the coupling g_4 has larger values for increasing magnetic field, as a consequence of the strong Coulomb repulsion between the currents localized at a given flank of the nanotube. The matrix element computed instead for electrons near opposite Fermi points (i.e. having opposite chiralities) gives the so-called g_2 coupling. The weak Coulomb repulsion between currents localized at antipodal points in the nanotube leads to relatively small values of g_2. This enters in the expression of the Luttinger liquid parameter

$$K = \sqrt{\frac{v_F + 2(g_4 - g_2)/\pi\hbar}{v_F + 2(g_4 + g_2)/\pi\hbar}} \tag{13}$$

which governs the low-energy transport properties [17]. The variation of K upon switching on the magnetic field, represented in figure 5, translates into a sharp decrease of the exponent α for the power-law behaviour of the tunnelling density of states, according to the relation $\alpha = (K + 1/K - 2)/8$ [6, 7]. The behaviour of the exponent, plotted in figure 5, provides a signature of the suppression of the electronic correlations in the presence of a transverse magnetic field [18], which seems to have been observed in the measurements of α in multi-walled nanotubes [19]. In the experiment reported in [19], it has actually been shown that a perpendicular magnetic field $B = 4$ T (with $R/2\pi\ell = 0.25$) is able to induce a reduction of the exponent α from 0.34 to 0.11, which is consistent with the reduction by a factor of $\approx$3 displayed in figure 5 for the parameters corresponding to the experiment.

6. Conclusions

To summarize, we have shown that, for thick carbon nanotubes in a transverse magnetic field, the transport properties are governed by the states localized at the flanks of the nanotube, which carry quantized currents in the longitudinal direction. Conversely, localized Landau states develop in the central region of the tube, where the component of the magnetic field

perpendicular to the surface is maximum. We observe at this point that the coexistence of a magnetic field and a Hall voltage, $V_{\rm H}$, may lead to an interesting realization of the setup discussed in [20], where an electric field (perpendicular to B) is also applied to the system. The Hall voltage gives rise to an electric field at the top and bottom regions of the nanotube, $\mathcal{E} \approx V_{\rm H}/R$. It has been shown that the Hall system with electric field undergoes a phase transition, similar to dielectric breakdown, for $\mathcal{E}/[(v_{\rm F}/c)B] = 1$ [20]. This corresponds to a current flowing along the nanotube,

$$I_c = \sigma_{xy} V_{\rm H}^c \sim 4nev_{\rm F}R/l^2.$$

The transition at higher bias currents leads to the suppression of the gaps between Landau levels, and it seems likely that, beyond this transition, the Hall conductance will no longer be quantized.

In any event, for nanotubes with a radius $R \approx 20$ nm in a magnetic field of ≈20 T, the band structure already shows a clear pattern of Landau levels. This opens the possibility of observing the quantization of the Hall conductivity in multi-walled nanotubes, where typically only the outermost shell is contacted by electrodes in transport experiments.

The presence of the plateaus in the Hall voltage should be fairly insensitive to the presence of moderate disorder in the nanotube samples, as long as the effect rests on the existence of chiral currents at opposite flanks of a nanotube. The overlap between states with currents flowing in opposite directions is exponentially small, so the chiral currents cannot suffer significant backscattering from impurities or lattice defects. It is only at the electrodes, where the chiral currents meet, that backscattering may appear. As is usually done in the context of the Hall effect in mesoscopic wires, this may be accounted for by means of a suitable transmission coefficient, that would reflect as an additional factor in the relation between the longitudinal current and the Hall voltage [21].

Finally, we remark that the absence of significant backscattering interactions must lead to good perspectives to measure the properties of a robust chiral liquid at the flanks of the nanotube, which could be accomplished by means of scanning tunnelling spectroscopy.

Acknowledgments

SB and PO acknowledge partial financial support from the grant 2006 PRIN Sistemi Quantistici Macroscopici-Aspetti Fondamentali ed Applicazioni di strutture Josephson Non Convenzionali. The financial support of the Ministerio de Educación y Ciencia (Spain) through grants FIS2005-05478-C02-01/02 is gratefully acknowledged. FG acknowledges funding from the European Union Contract 12881 (NEST). EP was supported by Consorzio Nazionale Interuniversitario per le Scienze Fisiche della Materia.

References

[1] Novoselov K S *et al* 2005 *Nature* **438** 197
[2] Zhang Y *et al* 2005 *Nature* **438** 197
[3] Peres N M R, Guinea F and Castro Neto A H 2006 *Phys. Rev.* B **73** 125411
[4] Gusynin V P and Sharapov S G 2005 *Phys. Rev. Lett.* **95** 146801
[5] Frank S *et al* 1998 *Science* **280** 1744
[6] Egger R and Gogolin A O 1997 *Phys. Rev. Lett.* **79** 5082
[7] Kane C, Balents L and Fisher M P A 1997 *Phys. Rev. Lett.* **79** 5086
[8] DiVincenzo D P and Mele E J 1984 *Phys. Rev.* B **29** 1685
[9] González J, Guinea F and Vozmediano M A H 1993 *Nucl. Phys.* B **406** 771
[10] Kane C L and Mele E J 1997 *Phys. Rev. Lett.* **78** 1932

[11] Saito R, Dresselhaus G and Dresselhaus M S 1998 *Physical Properties of Carbon Nanotubes* (London: Imperial College Press) chapter 6
[12] Bellucci S, González J, Onorato P and Perfetto E 2006 *Phys. Rev.* B **74** 045427
[13] McClure J W 1956 *Phys. Rev.* **104** 666
[14] Lee H-W and Novikov D S 2003 *Phys. Rev.* B **68** 155402
[15] Halperin B I 1982 *Phys. Rev.* B **25** 2185
[16] Perfetto E, González J, Guinea F, Bellucci S and Onorato P 2006 Quantum Hall effect in carbon nanotubes *Preprint* cond-mat/0604046
[17] Sólyom J 1979 *Adv. Phys.* **28** 201
[18] Bellucci S and Onorato P 2006 *Ann. Phys.* **321** 934
Bellucci S and Onorato P 2006 *Eur. Phys. J.* B **52** 469
[19] Kanda A *et al* 2004 *Phys. Rev. Lett.* **92** 36801
[20] Lukose V, Shankar R and Baskaran G 2006 *Preprint* cond-mat/0603594
[21] Büttiker M 1988 *Phys. Rev.* B **38** 9375